Self-Assembly

DOI: 10.1002/ange.200900639

Transition-Metal Phosphate Colloidal Spheres**

*Chen Chen, Wei Chen, Jun Lu, Deren Chu, Ziyang Huo, Qing Peng, and Yadong Li**

Colloidal spheres are frequently studied in materials science, chemistry, and biology[1] because their intrinsic properties can be tuned by changing parameters such as diameter, chemical composition, bulk structure, and crystallinity. To date, colloidal spheres have been widely used as fundamental building blocks in the fabrication of materials such as photonic bandgap (PBG) crystals (or photonic crystals),[2] two-dimensional crystalline arrays for masks in lithography, and three-dimensional macroporous materials.[3] The most-studied and best-established examples of such colloidal materials are silica and polymer colloids. Monodisperse silica colloids were first prepared by Stöber et al. in 1968 with a tetraethylorthosilicate (TEOS) hydrolyzing method;[4a] polymer colloidal spheres such as polystyrene (PS) and poly(methylmethacrylate) (PMMA) have been produced by emulsion polymerization.[5] During the past ten years, the scope of colloidal materials has been extensively broadened as the numbers of strategies for various semiconductor and metal colloidal spheres has increased. For example, semiconductor colloidal spheres with mesoscale dimensions (ZnS, CdS, a-Se, Ag_2Se, CdSe, and ZnO) have been successfully synthesized, although they tend to grow anisotropically into nonspherical structures.[6] Spherelike structures of Bi, Pb, In, Sn, Cd, and their alloys with melting points below 400 °C could also be conveniently prepared by using the bottom-up approach.[7] Our research group has studied colloidal spheres such as ZnSe hollow microspheres,[8] colloidal carbon spheres,[9] single-crystal Bi nanospheres,[10] magnetic single-crystal ferrite microspheres (Fe_3O_4, $MnFe_2O_4$, $ZnFe_2O_4$, and $CoFe_2O_4$)[11] and CeO_2–ZrO_2 nanocages.[12] We have developed a general emulsion-based bottom-up route to self-assemble various kinds of nanocrystals into three-dimensional colloidal spheres.[13] Since the scientific and technical potential of colloidal spheres is high, research into the synthesis of colloidal spheres can be fruitful. Herein, we report a new type of colloidal spheres: transition-metal phosphate colloidal spheres (TMPCS). An array of transition-metal (Mn, Fe, Co, Ni, and Cu) phosphate amorphous colloidal spheres was successfully synthesized by low-temperature solution-phase reactions. The colloidal spheres could crystallize upon annealing without obvious changes in morphology and size. The facility of the strategy means that the composition of the products can be well-controlled. Binary, ternary, and multinary composition phosphate colloidal spheres have been obtained, and the ratio of each component could be easily tuned. Moreover, iron phosphate hollow colloidal spheres could be obtained by adjusting the pH value of the system.

In a typical synthesis of copper phosphate colloidal spheres, the acidity of the phosphate ions resulted in a pH value of the initial mixed solution of approximately 2. Subsequent hydrolysis of the urea present in the solution led to a slow increase in the pH value. The reaction can be formulated as shown in Equation (1):

$$CO(NH_2)_2 + 2\,H^+ + H_2O \rightarrow 2\,NH_4^+ + CO_2 \quad (1)$$

A precipitate formed gradually as the pH value increased [Eq. (2)].

$$3\,Cu^{2+} + 2\,PO_4^{3-} \rightarrow Cu_3(PO_4)_2 \quad (2)$$

According to the LaMer diagram,[14] nucleation and growth processes were controlled by the slow hydrolysis. Colloidal spheres were then formed and protected by sodium dodecylsulfate (SDS) as capping ligand.

The scanning electron microscopy (SEM) images shown in Figure 1a,b reveal that the sample consists of colloidal spheres with diameters that range from 250 nm to 300 nm. Owing to the low temperature of the reaction, the colloidal spheres are amorphous, as confirmed by HRTEM images (Figure 1d). The dynamic light scattering (DLS) results (Figure 2a) show that the average hydrodynamic diameters of the spheres are about (250 ± 50) nm, which are consistent with the SEM results. Furthermore, the DLS results demonstrate that the colloidal spheres are stable and well-dispersed in solution. Zeta potential measurements (Figure 2b) indicate that these colloidal spheres have a negative surface charge (−17.1 mV), which suggests the presence of SDS on the particle surface. Energy dispersive spectrometry (EDS) analysis was utilized to determine the chemical composition of the colloidal spheres. As shown in Figure 2c, the sample is composed of only phosphorus, copper, gold, silicon, and oxygen (silicon is from the substrate; gold is coated on the surface of amorphous colloidal sphere to improve conductivity in SEM observations). The average atomic ratio of Cu/P is about 3:2, which is in good agreement with the predicted chemical formula. In order to further verify the chemical composition of the sample, the thermogravimetric analysis (TGA) curve was measured under a nitrogen atmosphere (see Figure S1a in the Supporting Information) From room temperature to 500 °C there is a gradual weight loss up to about 13.7 %, which can be attributed to the loss of chemically

[*] C. Chen, W. Chen, J. Lu, D. Chu, Z. Huo, Dr. Q. Peng, Prof. Y. Li
Department of Chemistry, Tsinghua University
Beijing, 100084 (P.R. China)
Fax: (+86) 10-6278-8765
E-mail: ydli@mail.tsinghua.edu.cn

[**] This work was supported by the NSFC (90606006), the State Key Project of Fundamental Research for Nanoscience and Nanotechnology (2006CB932300), and the Key Project of the Chinese Ministry of Education (grant no. 306020).

Supporting information for this article is available on the WWW under http://dx.doi.org/10.1002/anie.200900639.

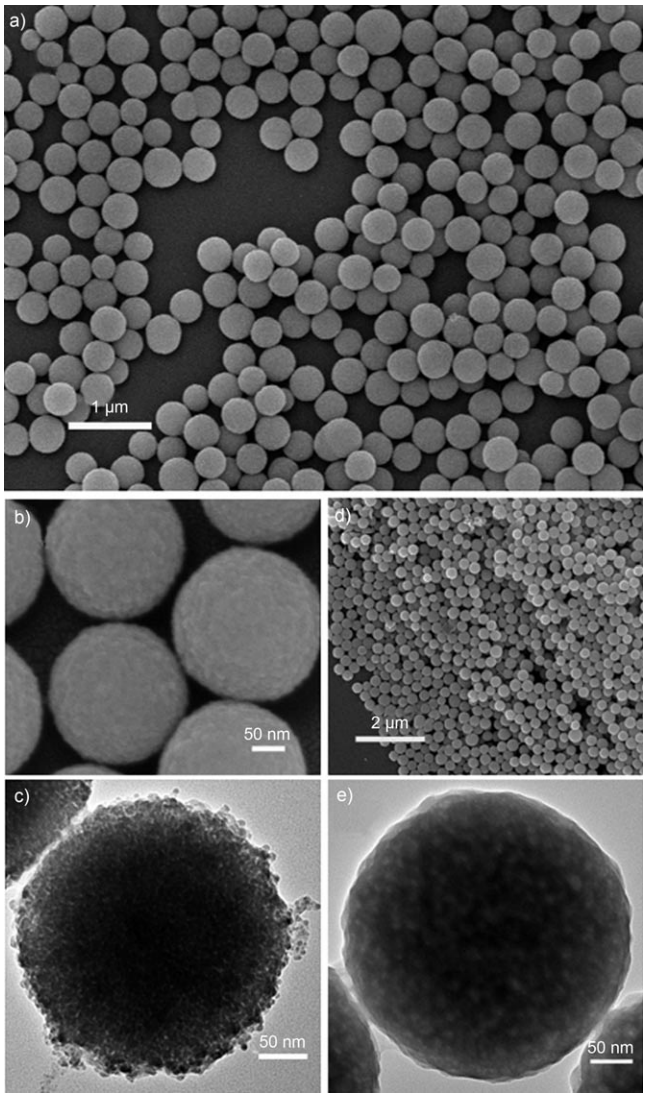

Figure 1. a, b) Typical SEM images and c) HRTEM image of the obtained copper phosphate colloidal spheres. d) A typical SEM image and e) HRTEM image of the copper phosphate colloidal spheres obtained after annealing at 500 °C.

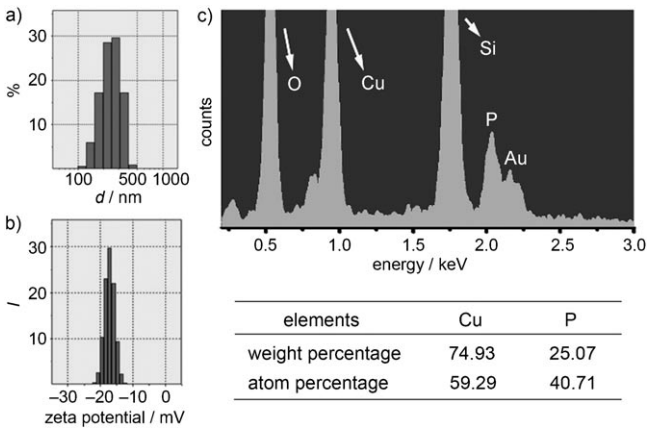

elements	Cu	P
weight percentage	74.93	25.07
atom percentage	59.29	40.71

Figure 2. a) DLS size-distribution diagram, b) zeta potential measurement, and c) EDS and element composition of the obtained copper phosphate colloidal spheres.

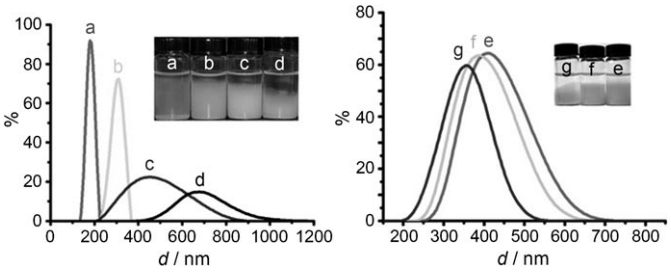

Figure 3. Size distributions of $Cu_3(PO_4)_2{\cdot}x\,H_2O$ colloidal spheres obtained by tuning the initial concentration of $CuSO_4$ in the synthesis: a) 3.2 mmol L^{-1}, b) 6.4 mmol L^{-1}, c) 9.6 mmol L^{-1}, and d) 12.8 mmol L^{-1}. Size distributions obtained by tuning the initial concentration of H_3PO_4: e) 0.12 mmol L^{-1}, f) 0.24 mmol L^{-1}, and g) 0.36 mmol L^{-1}. The insets show images of the samples after sedimentating for 2 days.

adsorbed water and hydroxy groups. We preliminarily speculated that the composition of the sample was $Cu_3(PO_4)_2{\cdot}x\,H_2O$; XRD measurements were carried out to confirm this conclusion. After annealing at 500 °C for 2 hours (see Figure S1b in the Supporting Information), the sample decomposed as $Cu_3(PO_4)_2$, thus confirming our hypothesis. The SEM and HRTEM images shown in Figure 1 d, e show no visible change in particle size and morphology after annealing at 500 °C. After annealing, the sample could be redispersed in deionized water by ultrasonication. When the annealing temperature was further raised to 800 °C, the sample was converted into copper pyrophosphate and copper oxide.

The size of the colloidal spheres can be easily controlled by adjusting the concentration of the precursor. The diameters of the copper phosphate colloidal spheres increased as the initial $CuSO_4$ concentration increased (Figure 3). A higher reactant concentration accelerated the growth process of the colloidal spheres, which resulted in an increased particle size. The concentration of surfactant did not increase with $CuSO_4$ concentration, which results in a probability increase of the collision and fusion of the particles. As a result, the size distribution became broader. However, the diameters of the colloidal spheres decreased as the H_3PO_4 concentration increased, as the pH value of the system was lowered and the precipitation process is decelerated.

This approach is powerful and general for the formation of phosphate colloidal spheres. Other transition-metal phosphate colloidal spheres can be easily obtained by changing the metal precursor. As shown in Figure 4 a–d, the SEM images and DLS results of TMPCSs synthesized with different precursors demonstrate that manganese phosphate, iron phosphate, cobalt phosphate, and nickel phosphate colloidal spheres have similar morphologies but different size distributions (the product of manganese phosphate consists of colloidal spheres and bulk precipitate; the DLS results show only the size distribution of colloidal spheres). After annealing at 500 °C, the phase identification of the as-synthesized TMPCSs was performed by using XRD (Figure S2 in the Supporting Information).

As mentioned above, the TMPCSs are amorphous colloidal spheres. Thus, binary TMPCSs can be simply

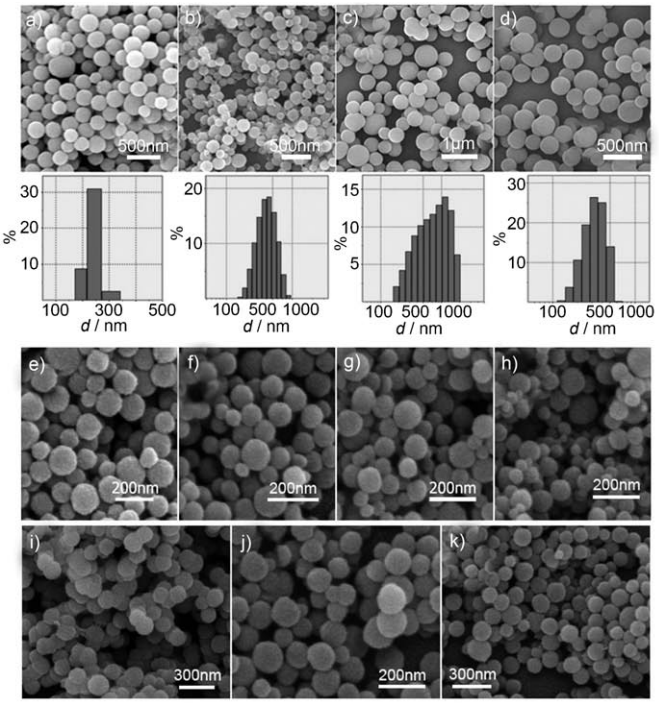

Image	Atom percentage Fe	Co	Ni	Cu	Mn
e	28.80	—	—	71.20	—
f	43.41	—	—	56.59	—
g	57.91	—	—	42.09	—
h	78.91	—	—	21.09	—
i	26.77	36.15	37.07	—	—
j	27.07	23.34	24.91	24.68	—
k	19.55	22.29	19.22	25.53	13.41

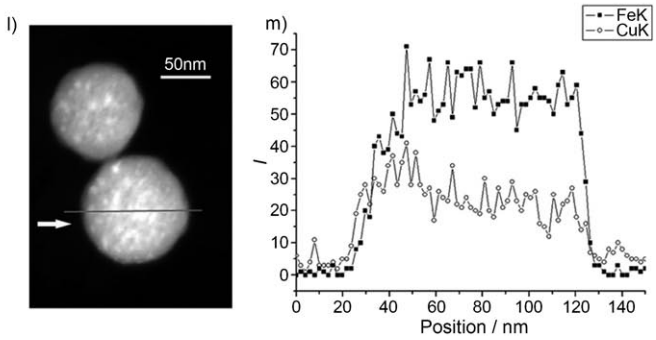

Figure 4. Typical SEM images of the obtained TMPCSs: a) manganese phosphate, b) iron phosphate, c) cobalt phosphate, and d) nickel phosphate. DLS size-distribution diagrams of each TMPCS are shown under the corresponding SEM images. SEM images of binary Fe–Cu TMPCSs tuned by the radio of the initial precursors ($CuSO_4$ and $(NH_4)_2Fe(SO_4)_2$): e) 1:4, f) 2:3, g) 3:2, and h) 4:1. SEM images of i) Fe–Co–Ni, j) Fe–Co–Ni–Cu, and k) Mn–Fe–Co–Ni–Cu TMPCSs. The calculated element radios of each component in obtained multinary TMPCSs are shown below the corresponding SEM images. l) The dark-field image of a single Fe–Cu TMPCS (molar ratio of Cu/Fe is 1:1.14); the gray line is the EDS line scanning route; m) compositional line profile across the nanostructure probed by EDS line scanning.

obtained by mixing two different precursors. Generally, the synthesis of multinary composition particles without lattice matching is difficult. In our case, lattice matching is not essential because of the amorphous characteristics of the products. A series of binary Fe–Cu TMPCSs with different radios of Fe and Cu are shown in Figure 4e–h. No visible difference is observed between the SEM images of the binary and unitary TMPCSs. However, the ratio of each component in binary TMPCSs can be tuned by changing the ratio of the metal precursors, as the molar ratio of the obtained colloidal spheres are approximately equal to the original reactant ratio according to the EDS analysis shown in Figure 4. The compositional line profile across a single colloidal sphere probed by EDS line scanning shown in Figure 4l,m reveals that both Fe and Cu were evenly distributed in colloidal spheres, that is, the as-obtained Fe–Cu binary TMPCS are homogeneous colloidal spheres. Representative synthesized multinary TMPCSs are listed in Table 1, and corresponding TEM images are given in Figure S4–6 in the Supporting Information.

Ternary, quaternary, and multinary TMPCSs were successfully synthesized by using this strategy. The SEM images of typical multinary TMPCSs (Fe–Co–Ni, Fe–Co–Ni–Cu, and Mn–Fe–Co–Ni–Cu) are shown in Figure 4i–k; a table of the molar ratios of each component is also given in Figure 4. The type and ratio of the components of TMPCSs can be selected readily. The total sort number of multinary TMPCSs calculated by permutation and combination [Eq. (3)] is 57.

$$\sum_{i=2}^{6} C(i,6) = C(2,6) + C(3,6) + C(4,6) + C(5,6) + C(6,6) = 57 \quad (3)$$

Interestingly, for iron phosphate, hollow colloidal spheres could be obtained (see TEM images in Figure 5a,b) when the initial concentration of H_3PO_4 was increased. In order to ascertain whether the pH value was the parameter responsible for the formation of hollow structures, sulfuric acid was added instead of increasing the original concentration of H_3PO_4. As the HRTEM images in Figure 5c,d show, hollow colloidal spheres formed with a higher initial concentration of sulfuric acid. A possible formation mechanism of these iron phosphate hollow colloidal spheres is discussed in the Supporting Information.

In summary, the TMPCSs reported herein are of great interest as they exhibit a range of structures and variable compositions, which are rarely observed in existing examples.

Table 1: Multinary TMPCSs.

Number of metals	Components	Particle size observed by TEM [nm]
2	Fe–Ni	200–300
	Fe–Mn	150–200
	Fe–Cu	100–200
	Co–Cu	200–250
	Mn–Cu	150–200
	Mn–Ni	200–350
	Ni–Cu	100–200
3	Fe–Mn–Ni	150–200
	Fe–Co–Ni	150–200
	Fe–Co–Cu	100–150
	Fe–Ni–Cu	50–150
	Mn–Ni–Cu	200–250
4	Fe–Co–Ni–Cu	50–150
	Mn–Fe–Co–Ni	150–200
5	Mn–Fe–Co–Ni–Cu	100–200
6	Mn–Fe–Co–Ni–Cu–Zn	150–200

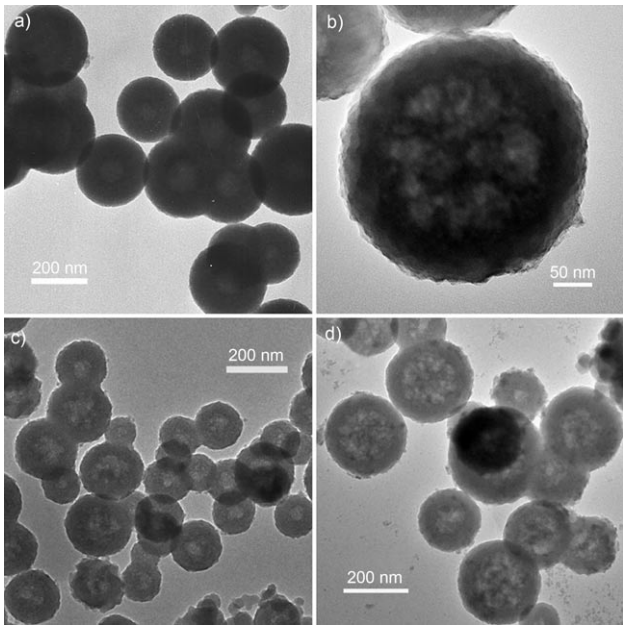

Figure 5. a) TEM image of iron phosphate hollow colloidal spheres obtained with quadruple original concentration of H_3PO_4. b) HRTEM image of above sample annealed at 500 °C. HRTEM images of iron phosphate hollow colloidal spheres obtained by adding c) 0.75 mmol H_2SO_4, and d) 3 mmol H_2SO_4 to the initial system.

Unitary (Mn, Fe, Co, Ni, and Cu) and several multinary (Fe–Ni, Co–Cu, Fe–Co–Cu, Fe–Co–Ni–Cu, Mn–Fe–Co–Ni–Cu, Mn–Fe–Co–Ni–Cu–Zn, etc) composition phosphate colloidal spheres and iron phosphate hollow spheres have been successfully synthesized by manipulating the initial stoichiometric ratios and pH values. Since transition-metal phosphates have many special properties because of the spatial arrangement of d-orbital electrons in transition metals, these newly developed TMPCSs significantly enrich the pool of available materials in the field of catalysis and lithium ion battery electrodes. It is believed that the established synthetic method could be extended to form other nanostructures that contain multiple transition-metal components.

Experimental Section

In a typical procedure, urea (6 g) and sodium dodecylsulfate (0.5 g) were dissolved in deionized water (100 mL). $CuSO_4$ or $MnSO_4$/$(NH_4)_2Fe(SO_4)_2$/$Co(NO_3)_2$/$NiSO_4$ (0.5 mmol) and the precursor H_3PO_4 (0.5 mmol) were added to the solution. The mixture was stirred until a homogeneous solution was formed, sealed in a teflon-lined stainless steel autoclave, and heated to 80 °C for 12 h. The products were separated by centrifugation at 4500 rpm for 5 min and redispersed in deionized water.

Two or more transition-metal salts were added into the above system to form corresponding multiple transition-metal phosphate colloidal spheres.

In a typical procedure for hollow transition-metal phosphate colloidal spheres, urea (6 g) and sodium dodecylsulfate (0.5 g) were mixed in deionized water (100 mL). $(NH4)_2Fe(SO_4)_2$ (0.5 mmol) and H_3PO_4 (2 mmol) were added to the mixed solution. The reaction temperature and time were the same as above.

Received: February 3, 2009
Revised: April 17, 2009
Published online: May 26, 2009

Keywords: colloids · emulsions · nanostructures · self-assembly · transition metals

[1] Y. Xia, *Adv. Mater.* **2000**, *12*, 693.
[2] a) W. L. Vos, R. Sprik, A. van Blaaderen, A. Imhof, A. Lagendijk, G. H. Wegdam, *Phys. Rev. B* **1996**, *53*, 231; b) I. I. Tarhan, G. H. Watson, *Phys. Rev. Lett.* **1996**, *76*, 315; c) I. I. Tarhan, M. P. Zinkin, G. H. Watson, *Opt. Lett.* **1995**, *20*, 1571; d) J. P. Ge, Y. D. Yin, *Adv. Mater.* **2008**, *20*, 3485.
[3] a) S. H. Park, Y. Xia, *Chem. Mater.* **1998**, *10*, 1745; b) S. H. Park, Y. Xia, *Adv. Mater.* **1998**, *10*, 1045; c) B. Gates, Y. Yin, Y. Xia, *Chem. Mater.* **1999**, *11*, 2827; d) S. A. Johnson, P. J. Ollivier, T. E. Mallouk, *Science* **1999**, *283*, 963; e) K. Kandori, H. Nakashima, T. Ishikawa, *J. Colloid Interface Sci.* **1993**, *160*, 499; f) K. Yoshino, S. B. Lee, S. Tatsuhara, Y. Kawagishi, M. Ozaki, A. A. Zakhidov, *Appl. Phys. Lett.* **1998**, *73*, 3506; g) R. Han, W. Pan, S. Shi, H. Wu, S. Liu, *Mater. Lett.* **2007**, *61*, 5014; h) J. F. Bertone, P. Jiang, K. S. Hwang, D. M. Mittleman, V. L. Colvin, *Phys. Rev. Lett.* **1999**, *83*, 300; i) P. Jiang, J. Cizeron, J. F. Bertone, V. L. Colvin, *J. Am. Chem. Soc.* **1999**, *121*, 7957; j) C. K. Tsung, J. Fan, N. F. Zheng, Q. H. Shi, A. J. Forman, J. F. Wang, G. D. Stucky, *Angew. Chem.* **2008**, *120*, 8810; *Angew. Chem. Int. Ed.* **2008**, *47*, 8682.
[4] a) W. Stöber, A. Fink, *J. Colloid Interface Sci.* **1968**, *26*, 62; b) J. N. Kuhn, W. Y. Huang, C. K. Tsung, Y. W. Zhang, G. A. Somorjai, *J. Am. Chem. Soc.* **2008**, *130*, 14026; c) L. Li, C. K. Tsung, T. Ming, Z. H. Sun, W. H. Ni, Q. H. Shi, G. D. Stucky, J. F. Wang, *Adv. Funct. Mater.* **2008**, *18*, 2956; d) R. Arshady, *Colloid Polym. Sci.* **1992**, *270*, 717.
[5] a) *Emulsion Polymerization* (Ed.: I. Piirma), Academic, New York **1982**; b) *Science and Technology of Polymer Colloids, Vol. II* (Eds.: G. W. Poehlein, R. H. Ottewill, J. W. Goodwin), Martinus Nijhoff, Boston, MA **1983**.
[6] a) K. P. Velikov, A. Van Blaaderen, *Langmuir* **2001**, *17*, 4779; b) E. Matijevic, D. Murphy-Wilhelmy, *J. Colloid Interface Sci.* **1982**, *86*, 476; c) U. Jeong, Y. Xia, *Adv. Mater.* **2005**, *17*, 102; d) U. Jeong, Y. Xia, *Angew. Chem.* **2005**, *117*, 3159; *Angew. Chem. Int. Ed.* **2005**, *44*, 3099; e) U. Jeong, J.-U. Kim, Y. Xia, *Nano Lett.* **2005**, *5*, 937; f) X. Hu, J. Gong, *Adv. Mater.* **2008**, *20*, 1; g) L. Li, C. K. Tsung, Z. Yang, G. D. Stucky, L. D. Sun, J. F. Wang, C. H. Yan, *Adv. Mater.* **2008**, *20*, 903.
[7] Y. Wang, Y. Xia, *Nano Lett.* **2004**, *4*, 2047.
[8] Q. Peng, Y. J. Dong, Y. D. Li, *Angew. Chem.* **2003**, *115*, 3135; *Angew. Chem. Int. Ed.* **2003**, *42*, 3027.
[9] X. Sun, Y. D. Li, *Angew. Chem.* **2004**, *116*, 607; *Angew. Chem. Int. Ed.* **2004**, *43*, 597.
[10] J. W. Wang, X. Wang, Q. Peng, Y. D. Li, *Inorg. Chem.* **2004**, *43*, 7552.
[11] H. Deng, X. Li, Q. Peng, X. Wang, J. Chen, Y. D. Li, *Angew. Chem.* **2005**, *117*, 2842; *Angew. Chem. Int. Ed.* **2005**, *44*, 2782.
[12] X. Liang, X. Wang, Y. D. Li, *J. Am. Chem. Soc.* **2008**, *130*, 2736.
[13] a) F. Bai, D. S. Wang, Z. Y. Huo, W. Chen, L. P. Liu, X. Liang, C. Chen, X. Wang, Q. Peng, Y. D. Li, *Angew. Chem.* **2007**, *119*, 6770; *Angew. Chem. Int. Ed.* **2007**, *46*, 6650; b) D. S. Wang, T. Xie, Q. Peng, Y. D. Li, *J. Am. Chem. Soc.* **2008**, *130*, 4016; c) D. S. Wang, T. Xie, Q. Peng, S. Y. Zhang, J. Chen, Y. D. Li, *Chem. Eur. J.* **2008**, *14*, 2507; d) D. S. Wang, T. Xie, Y. D. Li, *Nano Res.* **2009**, *2*, 30.
[14] E. M. Zaiser, V. K. LaMer, *J. Colloid Interface Sci.* **1948**, *3*, 571.
[15] Y. D. Yin, R. M. Rioux, C. K. Erdonmez, S. Hughes, G. A. Somorjai, A. P. Alivisatos, *Science* **2004**, *304*, 711.

